# Carbonation depth measurement of concretes exposed to different curing and preconditioning conditions, using image-processing tools

**Jessica C. Forsdyke[1] and Janet M. Lees[1]**

*[1]Department of Engineering,*
*University of Cambridge,*
*Civil Engineering Building, 7a JJ Thomson Ave, Cambridge, CB3 0FA, UK*

**Abstract**
Specimens of two concretes with different water/cement ratios are subject to various curing and pre-conditioning regimes before being placed in accelerated carbonation conditions. Their carbonation depths are revealed using a phenolphthalein indicator, with image-processing tools used to reduce measurement time, improve accuracy, and eliminate subjectivity of measurements. The results show that specimens cured in water for 28 days show a reduced carbonation depth when compared with those cured in air. Preconditioning with oven-treatment decreased the clarity in the observed carbonation front and had inconsistent effect on the carbonation depth. Image-processing tools were found to be a useful method of consistently measuring carbonation depth using a fixed threshold, particularly in this case where the indication is ambiguous.

## 1 Introduction

### 1.1 Concrete carbonation

Carbonation of concrete describes the process by which atmospheric $CO_2$ diffuses into concrete and reacts with hydration compounds within concrete pores in the presence of pore water. The result is a reduction in the pH of the material which can lead to loss of passivation of steel reinforcement and ultimately a reduction in the durability of reinforced concrete elements.

Carbonation is modelled using a variation of Fick's first law, where the depth of carbonated material, $x_c$, is proportional to the square root of exposure time, $t$:

$$x_c = K\sqrt{t} \tag{1}$$

This assumes that the rate of carbonation is diffusion controlled, such that the reaction time is not factored into the calculation of carbonation depth, and that there is no initial carbonation present ($x_{t=0} = 0$ ). The carbonation coefficient, $K$, captures the effect of a multitude of physical and chemical drivers for the rate of carbonation. Various models for $K$ in the literature predict it to be influenced by curing time, curing method, concrete mix design and microstructure as well as exposure conditions such as $CO_2$ concentration and relative humidity [1], [2].

### 1.2 Phenolphthalein indication of carbonation front

Since carbonation results in a decrease in pH of concrete from around 13 to around 8, a phenolphthalein indicator test is often employed to indicate the depth of carbonation, also known as the carbonation front. Phenolphthalein is an indicator solution which turns pink at a pH of above 9. Therefore, it can indicate the presence of carbonated and non-carbonated material when sprayed on a freshly exposed concrete surface. There is some debate in the literature over the accuracy of the phenolphthalein test in revealing the true location of carbonation front [3], [4]. However, it remains popular as a low cost, rapid test, which can be performed either in field or laboratory conditions without requirements for any other equipment. The phenolphthalein test has long provided a relative indication of the extent of carbonation, informing engineers about the longevity of concrete structures.

Research has suggested that the clarity of the carbonation front obtained from a phenolphthalein test can also be affected by phenomena such as preconditioning. Turcry et al. [5] discovered that in 50% $CO_2$ accelerated testing, there was an initial "double front" indicated by the phenolphthalein for

specimens which had been preconditioned by oven drying prior to $CO_2$ exposure. Oven preconditioned specimens show a zone near the surface which is behind the true carbonation front but remains at a pH<9. This phenomenon may be attributed to high temperatures causing the chemically bonded water molecules in the concrete to be removed and leaving a very low water content at the surface of the material. In this low humidity zone, although $CO_2$ can diffuse through, there is not enough pore water to facilitate complete carbonation reactions in the concrete pores. Therefore, the required pH for colour change in the indicator solution is still maintained and some material near the surface is not fully carbonated, as shown in Figure 1.

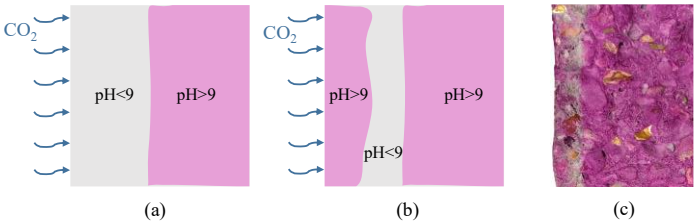


Fig. 1 Adapted from Turcry et al. [5] showing the carbonation front appearance in (a) standard specimens and ((b) and (c)) preconditioned specimens

Figure 2 (a) shows a clear, easy to measure carbonation front indicated by the phenolphthalein solution, which is not always the case. Carbonation fronts from phenolphthalein testing can be difficult to determine if a highly porous concrete mix is cast, as shown in Figure 2 (b), where the line of pink indication is ambiguous. Very low carbonation depth values can often also be difficult to detect by eye due to the high precision required, as shown in Figure 2 (c).

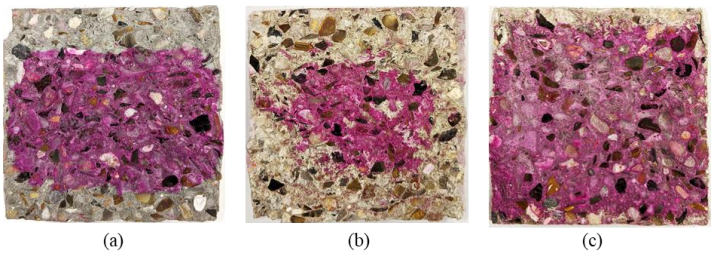


Fig. 2 Clear carbonation front (a) compared to ambiguous carbonation fronts due to high porosity (b) or low absolute value (c)

### 1.3 Image processing

When measuring the carbonation front after $CO_2$ exposure, an internal concrete surface is revealed by splitting of the material. This is then sprayed with a phenolphthalein solution, and the distance from the edge exposed to carbonation and the pink indication is traditionally measured using calipers to obtain the carbonation depth value.

By nature, concrete is not a completely homogeneous material due to the presence of aggregates embedded in the mortar. Therefore, the carbonation front is not a perfectly straight line. Taking an average of the carbonation depth measured at multiple locations is often used to reduce variability of results. The method proposed by BS 1881-210:2013 [6] suggests taking measurements at 5 regular intervals on each exposed face of a test specimen. However, this process can be time-consuming, is very difficult when carbonation fronts are extremely small, and does not provide the full scope of information about the shape, deviation, or maximum penetration of the carbonation front.

Giulietti et al. [7] embraced image-processing tools as a method to overcome these limitations of measurement by hand. They found a correlation of $R^2$=0.96 between results measured using these methods when compared to those measured with callipers. Their method made use of thresholding of images in the hue, saturation, value (HSV) colour space to detect both the region of interest (the concrete face) and the pink uncarbonated zone indicated by the phenolphthalein solution. Advanced features made use of machine learning to filter out anomalous points due to large aggregates. The distance between the

carbonation front and specimen edge was then calculated. Results were calibrated from pixels to absolute distances using detection of ArUco markers in the images which were adjacent to the concrete face in the images. Previous research by Choi et al.[8], Segura et al. [9] and Ruiz Madera [10] has also demonstrated successful application of image processing to determine the carbonation depth from the phenolphthalein indication test.

Image processing is beneficial for carbonation depth measurement as it implements an objective threshold value which is uniform across concretes of the same colour photographed in the same lighting. This is favourable to the subjective human eye, which may exhibit bias or have difficulty in determining the carbonation depth when it is unclear for any of the reasons mentioned previously.

## 2 Method

An experimental programme was designed to test the carbonation behaviour of concretes subjected to different curing and preconditioning conditions. The carbonation depth was obtained for these experiments using image processing tools.

### 2.1 Accelerated carbonation tests

In this study, a total of eight 100 × 100 × 100 mm cube specimens of two different concretes were exposed to accelerated carbonation testing in a chamber at 4% $CO_2$ concentration, 20°C and 55% relative humidity for a total of 3 weeks. The general method followed in preparation and testing of specimens was that of BS 1881-210:2013 [6].

Two mixes were selected for this study, with water/cement ratios of 0.6 and 0.8. These mixes are referred to as A0.6 and B0.8 respectively. Their compositions are given in Table 1. A small amount of black mortar dye was used in B0.8 to improve differentiation between specimens. The mixes used CEMI 52.5 N cement, which comprises of 90% Clinker, 5.2% Limestone, 4.6% Gypsum and 0.2% Ferrous Sulphate [11]. The compressive strength of the mixes is the average of three cubes of dimension 100 × 100 × 100 mm, measured after 28 days of wet curing.

Table 1 Mix designs of mixes used in experimental program

| Material | Units | A0.6 | B0.8 |
|---|---|---|---|
| Cement; 52.5 N CEM I | [kg/m$^3$] | 325 | 225 |
| Coarse aggregate; 0-10 mm gravel | [kg/m$^3$] | 700 | 794 |
| Fine aggregate; 0-4 mm sand | [kg/m$^3$] | 1199 | 1248 |
| Water | [kg/m$^3$] | 197 | 180 |
| Black mortar dye | [kg/m$^3$] | - | 4.5 |
| *w/c* | [-] | 0.60 | 0.80 |
| *a/c* | [-] | 5.84 | 9.07 |
| $f_{cube}$ | [MPa] | 32.2 | 48.5 |

To test the effect of the curing and preconditioning on the carbonation behaviour of the concretes, specimens were subjected to different regimes before being exposed to accelerated carbonation conditions at the same age. All specimens remained in moulds for their initial setting period of 24 hours, before being transferred to their curing locations in the laboratory (air curing) or water tank (wet curing), followed by preconditioning in laboratory or laboratory+oven conditions. “Laboratory conditions” refer to an environment of 20±2°C and 60±5% relative humidity, whereas “oven conditions” refer to an oven environment of 105°C and low humidity. Preconditioning is a necessary step in accelerated carbonation tests as it ensures specimens are fully dry prior to introduction to the carbonation environment, where excess pore water may affect the rate of carbonation.

The four different overall regimes are summarised in Table 2. Regimes I and II were wet cured, III and IV were air cured. Regimes II and IV were preconditioned in the laboratory only, and I and III were

preconditioned in the laboratory and oven. One cube from each mix was exposed to each of the four different regimes prior to accelerated carbonation.

Table 2 Curing and preconditioning regimes, each applied to one cube of each mix

| Regime | Initial setting [days] | Wet curing [days] | Air curing [days] | Laboratory conditioning [days] | Oven conditioning [days] | Carbonation at 4% $CO_2$ [days] |
|---|---|---|---|---|---|---|
| I | 1 | 27 | - | 11 | 3 | 21 |
| II | 1 | 27 | - | 14 | - | 21 |
| III | 1 | - | 27 | 11 | 3 | 21 |
| IV | 1 | - | 27 | 14 | - | 21 |

Four faces of the specimens were sealed after curing was complete using paraffin wax, to prevent ingress of $CO_2$ into all but two opposing faces. In all cases, the faces exposed to carbonation were formed faces (cast against the side of plastic formwork) which had no other treatment applied before exposure.

After 3 weeks of exposure in the carbonation chamber, the specimens were removed and split using a tensile splitting apparatus. The freshly split surface was then sprayed with a fine mist of a solution of 1% phenolphthalein in ethanol to reveal the carbonation front. The specimens were then photographed using a high-resolution DSLR camera under LED lighting and against a white background, to prevent shadows and maximise the likelihood of detecting the carbonation front correctly.

## 2.2 Image processing

Image processing to extract carbonation depth from photographs in this study was carried out using Matlab software, utilising the Image Processing Toolbox. CIELAB colour space (also known as L*a*b* colour space) thresholding was used to detect the edge of carbonation specimens and the edge of the pink region. This colour space was chosen since it demonstrated the most consistent pink colour detection, when compared to HSV and RGB. Since the specimens are known to be 100 × 100 mm, values were calibrated from pixels to true distances using these average dimensions of the face as reference.

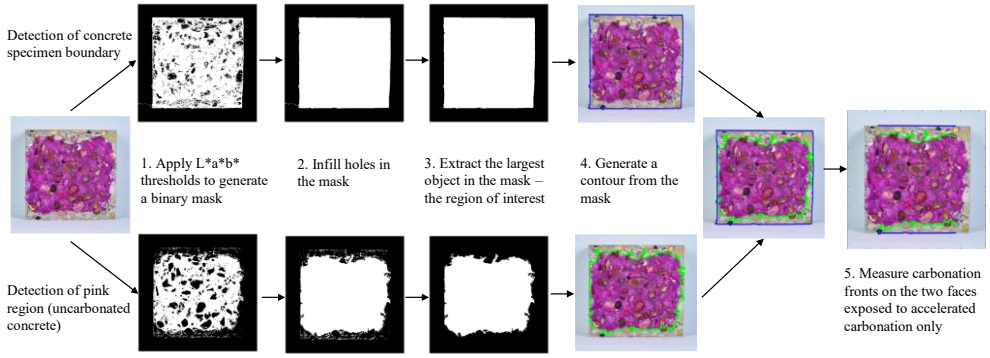


Fig. 3 Image processing used to detect carbonation fronts on faces exposed to accelerated carbonation (top and bottom faces of specimen shown)

The flow chart in Figure 3 details the thresholding and filters applied to extract the location of the carbonation front from any given photograph. An a* (position between green and red) threshold is applied to detect the pink region since the colour falls distinctly on one end of this spectrum, whereas an L* (lightness) threshold is applied to detect the edge of the specimen since this can discriminate based on brightness and therefore detect a white background.

## 3 Results and Discussion

Carbonation depths measured after 3 weeks of exposure in 4% $CO_2$ environment are presented in this section. The influence of curing conditions, and preconditioning are assessed, as well as the effectiveness of the image processing method used in detecting the carbonation depth.

### 3.1 Carbonation depths

Using the image processing method described in Figure 3, the carbonation depth has been extracted from photographs. For completeness of information, the maximum and minimum measured values for each front, and standard deviation of carbonation depth are also extracted and presented in Table 3. The carbonation coefficient is calculated using equation 1.

Table 3 Measured carbonation depths of specimens

| Mix | Regime | Average carbonation depth, $x_c$ [mm] | Maximum [mm] | Minimum [mm] | Standard deviation [mm] | Carbonation coefficient, $K$ [mm/day$^{1/2}$] |
|---|---|---|---|---|---|---|
| A0.6 | I | 7.1 | 12.9 | 2.9 | 1.9 | 1.6 |
| | II | 6.2 | 13.1 | 0.0 | 2.7 | 1.3 |
| | III | 10.8 | 19.5 | 1.9 | 2.7 | 2.4 |
| | IV | 10.1 | 16.2 | 5.1 | 2.2 | 2.2 |
| B0.8 | I | 7.5 | 15.9 | 0.0 | 3.0 | 1.6 |
| | II | 6.8 | 11.9 | 1.8 | 2.1 | 1.5 |
| | III | 8.6 | 15.2 | 3.6 | 2.0 | 1.9 |
| | IV | 16.8 | 22.7 | 12.3 | 2.2 | 3.7 |

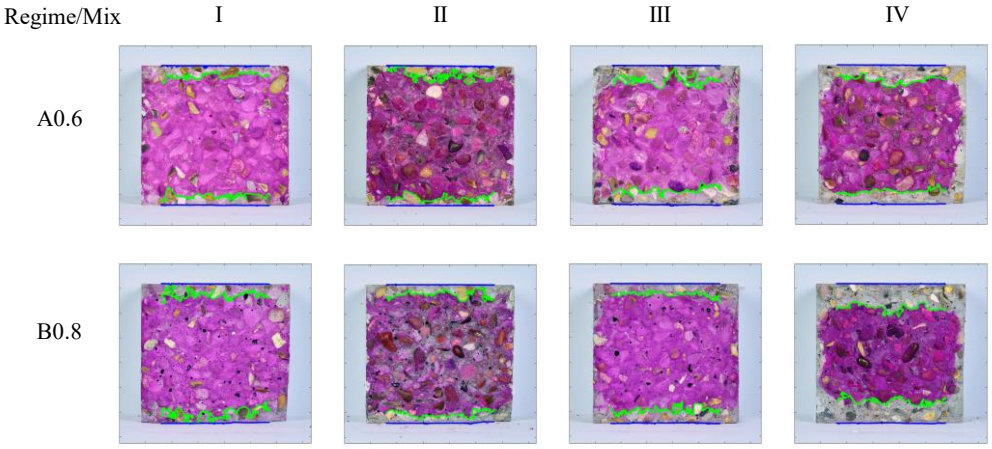


Fig. 4 Photographs of all specimens with detected carbonation fronts highlighted in green and face boundaries highlighted in blue

Overall, carbonation depths ranging from 0.0 to 22.7 mm were measured in the specimens after exposure to 4% $CO_2$ concentrations for a period of 3 weeks. The detected carbonation fronts exhibited variability due to aggregates impeding carbonation, as can be seen by the fluctuations in all the carbonation fronts indicated in green in Figure 4. The standard deviations remain consistent across the regimes and mixes, at around 2 mm. The results show that for the mixes and conditions assessed here, the curing and preconditioning regime appears to have a greater influence on the final carbonation depth than the w/c ratio of the mix, since the carbonation depths for one mix are not consistently higher than another.

### 3.1.1 Effect of curing conditions on carbonation

Specimens were subject to two different curing methods in this study: wet curing (regimes I and II) or air curing (regimes III and IV) until 28 days from casting had passed. The results in Table 3 and Figure 4 demonstrate that specimens cured in air carbonated on average 4.7 mm deeper than their counterparts with the same preconditioning cured in water. This is consistent with findings of Balayssac, Détriché, and Grandet [12], and Ding et al. [13] who all observed than longer periods of water curing decreased carbonation depths in accelerated carbonation tests.

It may be noted that during the initial curing and conditioning period, the specimens which were held in laboratory conditions were exposed to atmospheric $CO_2$ concentrations of around 0.04%, 100 times less than the accelerated conditions of the test. It is therefore possible that there was some carbonation of these specimens prior to their introduction to the accelerated environment. However, it is widely thought that the carbonation resistance, *K*, is proportional to the square root of $CO_2$ concentration [14]. Equation 2 can therefore be applied for conversion.

$$K_{0.04\%} = K_{4\%}\sqrt{\frac{0.04}{4}} = 0.32\,K_{4\%} \tag{2}$$

The following calculation for A0.6.II and A0.6.IV demonstrates that any carbonation which occurred in the 28-day air curing stage would be insufficient to account for the 3.8 mm increase in carbonation depth of air cured (A0.6.IV) compared to water cured (A0.6.II) specimens.

$$x_{0.04\%} = K_{0.04\%}\sqrt{t} = 0.32 \times 1.3 \times \sqrt{28} = 2.25 \text{ mm} \tag{3}$$

### 3.1.2 Effect of preconditioning

Two different preconditioning methods were tested in this work. Specimens were either held in laboratory conditions for 14 days (regimes II and IV) or conditioned in laboratory conditions for 11 days and in oven conditions for 3 days (regimes I and III).

As can be seen in Figure 4, oven preconditioned specimens (I and III for both mixes) displayed an indication which was a much lighter shade of pink. This was also true of the concrete before it was sprayed with indicator solution, when it appeared much drier than the concretes preconditioned in laboratory conditions only.

The carbonation depths appeared slightly higher (<1 mm) for the majority of oven preconditioned specimens (I and III) compared to their corresponding laboratory preconditioned specimens (II and IV). However, in the B0.8 specimens which were cured in air (B0.8.III and B0.8.IV), the application of oven preconditioning in B0.8III appears to have significantly slowed the rate of carbonation.

Overall, concerns about oven preconditioning (sometimes referred to as oven drying) arise because high temperatures, such as 105°C used in this case, can remove both free and physically bound water from concrete. Dehydration of gypsum begins around 80°C and decomposition of ettringite begins around 60°C [15], leading to chemical changes at high temperatures. Physical changes to the pore structure due to oven drying are well documented [15]–[17]. Since carbonation reactions take place in concrete pores and rely on the presence of an optimal amount of pore water, any of these effects may alter the carbonation behaviour of a concrete mix.

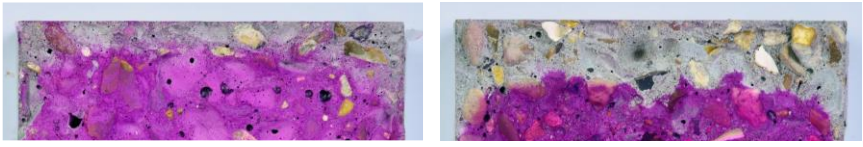

(a) B0.8.III (b) B0.8.IV

Fig. 5 Difference in clarity of carbonation front seen in (a) oven-preconditioned and (b) laboratory preconditioned specimens of mix B0.8 cured in air.

In this investigation the most noticeable effect of oven preconditioning was on the definition and clarity of the carbonation front. The fronts in oven-preconditioned specimens (I and III) were much less well defined than those in specimens which were kept in laboratory conditions throughout, as seen in

Figure 5. There is notable blurring of the interface between the uncarbonated and carbonated zones, and some pink indication remaining in the carbonated zone. This makes detection of the carbonation front more difficult when measured manually and highlights an area where objective colour thresholds from image processing tools can be used to ensure consistency in the measurement of carbonation depth across preconditioned specimens.

### 3.2 Use of Image processing

It is clear from visual inspection of Figure 5 that the image processing tools used in this work have been successful in locating and measuring the carbonation fronts in the specimens tested. Added benefits of this process over traditional manual measurements were that, once the program was written and photographs uploaded, the carbonation front could be obtained quickly and efficiently for as many specimens as required. More information about the carbonation front is obtained by measuring thousands of data-points in this way instead of only a few measured manually. Therefore, the average carbonation depth is less likely to be influenced by anomalous points, improving accuracy, and the standard deviation of carbonation depth can be calculated.

Another major benefit to this method was the elimination of subjectivity of measurements, particularly when carbonation depths are not clear, as in Figure 5. In all cases, the same thresholds were able to be used to generate masks for detecting the pink region or boundary of the concrete faces, so carbonation front detection was consistent. Some iteration was required to find the exact threshold values which would be universally successful. It was observed that robustness of this process could be improved by changing the colour of the background in future to one which is not found in concrete, such as green. It was occasionally difficult to isolate the white background from some of the lighter coloured aggregates in the concrete specimens.

Overall, confidence in measurement of a variable phenomenon such as carbonation can be improved dramatically using image processing tools.

## 4 Conclusions

In this work, accelerated carbonation tests were carried out on two different concrete mixes of w/c 0.6 or 0.8 exposed to four different curing and preconditioning regimes. For the conditions and materials assessed, the influence of curing regime on carbonation depth appears to be greater than the influence of the w/c ratio.

The results showed that the method of preconditioning, whether oven-treatment or laboratory conditioning, had an inconsistent effect on the measured carbonation depth. However, oven preconditioning was shown to make the carbonation front significantly more difficult to visually identify; highlighting the need for unbiased digital measurement methods such as the image processing technique presented in this work.

The curing method was found to have a significant influence on the carbonation depth of specimens of both concrete mixes. The carbonation depth in air cured specimens was, on average, 4.7 mm higher than their water-cured counterparts subject to the same preconditioning.

Edge detection using CIELAB colour space thresholding and further refinement filters was found to be effective in detecting the carbonation front and face boundary on specimens sprayed with phenolphthalein indicator solution. This method gave a greater degree of information about the nature of carbonation fronts than would be achieved by manual measurement. The technique was particularly useful in cases where the carbonation depth was poorly defined.

## Acknowledgements

The authors would like to acknowledge funding from the Engineering and Physical Sciences Research Council (UK) through the EPSRC Established Career Fellowship titled ‘‘Tailored Reinforced Concrete Infrastructure: Boosting the Innate Response to Chemical and Mechanical Threats” [reference number: EP/N017668/1] and the Doctoral Training Partnership [reference number: EP/N509620/1]. Thanks are extended to technical staff at the Civil Engineering Department, University of Cambridge, for their support in the experimental programme and to other members of the Concrete Infrastructure Research Group: Dr Michele W.T. Mak, Mar Gimenez Fernandez, Dr Marcus Maier, Hasini Weerasinghe and Harry Edwards, for their advice and comments in exploration of ideas for this work.

## References


[1] J. C. Forsdyke and J. M. Lees, "An Analysis of Existing Models for Carbonation Coefficient Applied to Tests under Natural Conditions," in *fib Symposium 2021: Concrete Structures: New Trends for Eco-Efficiency and Performance*, 2021.

[2] Q. Qiu, "A state-of-the-art review on the carbonation process in cementitious materials: Fundamentals and characterization techniques," *Constr. Build. Mater.*, vol. 247, p. 118503, 2020, doi: 10.1016/j.conbuildmat.2020.118503.

[3] C. F. Chang and J. W. Chen, "The experimental investigation of concrete carbonation depth," *Cem. Concr. Res.*, vol. 36, no. 9, pp. 1760–1767, Sep. 2006, doi: 10.1016/j.cemconres.2004.07.025.

[4] S. Chatterji, K. A. Snyder, and J. Marchand, "Depth profiles of carbonates formed during natural carbonation," *Cem. Concr. Res.*, vol. 32, no. 12, pp. 1923–1930, Dec. 2002, doi: 10.1016/S0008-8846(02)00908-0.

[5] P. Turcry, L. Oksri-Nelfia, A. Younsi, and A. Aït-Mokhtar, "Analysis of an accelerated carbonation test with severe preconditioning," *Cem. Concr. Res.*, vol. 57, pp. 70–78, 2014, doi: 10.1016/j.cemconres.2014.01.003.

[6] British Standards Institution, "BS 1881-210:2013 Testing hardened concrete Part 210 : Determination of the potential carbonation resistance of concrete - Accelerated carbonation method," 2013.

[7] N. Giulietti *et al.*, "Automated measurement system for detecting carbonation depth: Image-processing based technique applied to concrete sprayed with phenolphthalein," *Meas. J. Int. Meas. Confed.*, vol. 175, no. January, p. 109142, 2021, doi: 10.1016/j.measurement.2021.109142.

[8] J.-I. Choi, Y. Lee, Y. Y. Kim, and B. Y. Lee, "Image-processing technique to detect carbonation regions of concrete sprayed with a phenolphthalein solution," *Constr. Build. Mater.*, vol. 154, pp. 451–461, 2017, doi: 10.1016/j.conbuildmat.2017.07.205.

[9] I. Segura, M. Molero, S. Aparicio, and A. Moragues, "Measurement of the degraded depth in cementitious materials by automatic digital image processing," *Meas. Sci. Technol.*, vol. 21, no. 5, 2010, doi: 10.1088/0957-0233/21/5/055103.

[10] C. C. Ruiz Madera, "Implementación de algoritmos de inteligencia artificial y procesamiento digital de imágenes en la determinación de la profundidad de carbonatación en estructuras de concreto," Universidad Militar Nueva Granada, 2018.

[11] BRE and Hanson UK, "Environmental Product Declaration - Hanson Bulk CEM I," no. 000242, 2019.

[12] J. P. Balayssac, C. H. Détriché, and J. Grandet, "Effects of curing upon carbonation of concrete," *Constr. Build. Mater.*, vol. 9, no. 2, pp. 91–95, 1995, doi: 10.1016/0950-0618(95)00001-V.

[13] S. Ding, Z. Shui, T. Pan, W. Chen, and W. Xu, "Effects of Curing Conditions on Carbonation of Concrete Containing Expansive Admixture," in *The 2013 World Congress on Advances in Streuctural Engineering and Mechanics (ASEM13), Jeju, Korea, September 8-12, 2013*, 2013, pp. 3298–3312.

[14] E. I. Moreno, "Carbonation coefficients from concrete made with high-absorption limestone aggregate," *Adv. Mater. Sci. Eng.*, vol. 2013, 2013, doi: 10.1155/2013/734031.

[15] C. Gallé, "Effect of drying on cement-based materials pore structure as identified by mercury intrusion porosimetry - A comparative study between oven-, vacuum-, and freeze-drying," *Cem. Concr. Res.*, vol. 31, no. 10, pp. 1467–1477, 2001, doi: 10.1016/S0008-8846(01)00594-4.

[16] M. Moukwa and P. C. Aitcin, "The effect of drying on cement pastes pore structure as determined by mercury porosimetry," *Cem. Concr. Res.*, vol. 18, no. 5, pp. 745–752, 1988, doi: 10.1016/0008-8846(88)90098-1.

[17] A. Korpa and R. Trettin, "The influence of different drying methods on cement paste microstructures as reflected by gas adsorption: Comparison between freeze-drying (F-drying), D-drying, P-drying and oven-drying methods," *Cem. Concr. Res.*, vol. 36, no. 4, pp. 634–649, 2006, doi: 10.1016/j.cemconres.2005.11.021.